



Noise generation and propagation by biomimetic dynamic-foil thruster

Kostas Belibassakis¹ and Iro Malefaki²

School of Naval Architecture & Marine Engineering,
National Technical University of Athens, Greece

Email: kbel@fluid.mech.ntua.gr⁽¹⁾, iromalefaki@gmail.com⁽²⁾

Abstract

Biomimetic flapping-foil thrusters are able to operate efficiently while offering desirable levels of thrust required for the propulsion of a small vessel or an Autonomous Underwater Vehicle (AUV). Extended review of hydrodynamic scaling laws in aquatic locomotion and fishlike swimming can be found in Triantafyllou et al (2005). Flapping-foil configurations have been investigated both as main propulsion devices and for augmenting ship propulsion in waves; see also the review by Wu et al (2020). In this work biomimetic systems are studied with application to small vessel or AUV propulsion and their comparative performance with standard marine propellers concerning the reduction of noise. A three-dimensional model of the lifting flow around the dynamic foil is presented and its application is discussed as regards the prediction of the hydrodynamically generated noise, in conjunction with methods allowing for the calculation of acoustic propagation and spatial evolution of the spectrum, based on data concerning the noise sources on the dynamic foil, coupled with the solution of the hydroacoustic problem.

Keywords: Biomimetic flapping-foil thrusters, small vessel / AUV propulsion, hydrodynamic noise

1 Introduction

The seas become substantially noisier the last decades and anthropogenic sources contribute substantially in this degradation trend with detrimental effects on sea life and particularly on marine mammals; see, e.g., Duarte et al (2021). Shipping, resource exploration, and infrastructure development have increased the anthropophony (sounds generated by human activities), whereas the biophony (sounds of biological origin) has been reduced by hunting, fishing, and habitat degradation. In particular, shipping noise has a significant impact on the marine environment as demonstrated by the fact that at low frequencies below 300 Hz, ambient noise levels have been increased by 15-20dB over the last century (McKenna et al 2012).

Many recent studies have shown that underwater-radiated noise from commercial ships may have both short and long-term negative consequences on marine life, especially marine mammals. The issue of underwater noise and impact on marine mammals was first raised at IMO in 2004. It was noted that continuous anthropogenic noise in the ocean was primarily generated by shipping. Since ships routinely cross international boundaries, management of such noise required a coordinated international response.

Moreover, in 2008, the IMO Marine Environment Protection Committee (MEPC) agreed to develop non-mandatory technical guidelines to minimize the introduction of incidental noise from commercial shipping operations into the marine environment to reduce potential adverse impacts on marine life.

As far as the radiated noise is concerned, it has been found that different components are dominant at different speeds. In particular, hydrodynamic noise due to propeller operation in the wake of the ship and machinery is dominant at low speeds, whereas propeller noise is dominant at higher speed especially when cavitation takes place; see also Belibassakis (2018). Marine propellers are the standard devices used for ship propulsion and are characterized by increased load distribution on the disc while operating at high rotational speed conditions. The increased flow speed is the main reason leading to the appearance in almost all cases of partial cavitation manifested near the tip region and occasionally also at the hub of marine propeller blades and the trailing vortex sheets. The fast variation of the generated bubble cavitation volume on the propeller blades, acting as acoustic monopole terms, in conjunction with dipole contribution due to unsteady blade load, leads to the generation of intensive noise, especially at the blade frequency and the first harmonics, while at higher frequencies noise is caused by sheet cavity collapse and shock wave generation; see also Seol et al (2005). In the lower frequency band, the noise excitation from marine propeller, especially under partial cavitating conditions, match well the first octave bands, which has negative impact on the life conditions particularly of marine mammals. On the other hand, flapping-foil thrusters are systems operating at substantial lower frequency as compared with marine propellers and are characterized by much smaller power concentration. The latter biomimetic devices are able to operate very efficiently while offering desirable levels of thrust required for the propulsion a small vessel or an Autonomous Underwater Vehicle (AUV); see, e.g., Triantafyllou et al (2000), Rozhdestvensky & Ryzhov (2003). Extended review of hydrodynamic scaling laws in aquatic locomotion and fishlike swimming can be found in Triantafyllou et al (2005). Moreover, flapping-foil configurations have been investigated both as main propulsion devices and for augmenting ship propulsion in waves, substantially improving the performance by exploitation of renewable wave energy. More details can be found in Belibassakis & Politis (2013), Belibassakis & Filippas (2015); see also the review Wu et al (2020). In the framework of Seatech H2020 project entitled “Next generation short-sea ship dual-fuel engine and propulsion retrofit technologies” (<https://seatech2020.eu/>) a concept of symbiotic ship engine and propulsion innovations is studied, that when combined, are expected to lead to significant increase in fuel efficiency and emission reductions. The proposed renewable-energy-based propulsion innovation is based on the bio-mimetic dynamic wing, mounted at the ship bow to augment ship propulsion in moderate and higher sea states, capturing wave energy and producing extra thrust while damping ship motions.

In this work biomimetic flapping thrusters are considered with application to the propulsion of small vessel and AUV and approximate models are presented in order to evaluate their comparative performance with standard marine propellers concerning the reduction of noise. More specifically, a three-dimensional model of the lifting flow around the dynamic foil operating as an unsteady flapping thruster is described. The method is based on vortex-ring elements and its application is subsequently presented concerning the prediction of the dynamical behavior of the system and the hydrodynamically generated noise. Finally results are presented showing the effectiveness of the model to be used, in conjunction with methods allowing for the calculation of acoustic propagation and spatial evolution of the acoustic spectrum, based on data concerning the noise sources on the dynamic foil, coupled with the solvers of the hydroacoustic problem.

2 The vortex ring element method for flapping thruster performance

A vortex ring element method based on quadrilateral elements will be used to discretize the wing and its trailing vortex wake and the singularity strengths are calculated to satisfy directly the no-entrance boundary condition on the surface of the foil, along with the Kutta condition. A general foil geometry is modelled including camber, thickness and various planform shapes and aspect ratio $AR=s^2/A$, where s is the span of the wing, c the midchord length and A the planform area. A main difference with the lifting surface Vortex-Lattice model (Katz & Plotkin 1990), is that the exact boundary condition is satisfied on the actual wing surface, in contrast with lifting surface models where the boundary condition is satisfied on the mean camber surface and the thickness effects are taken into account by linearization procedure and a corresponding source-sink lattice.

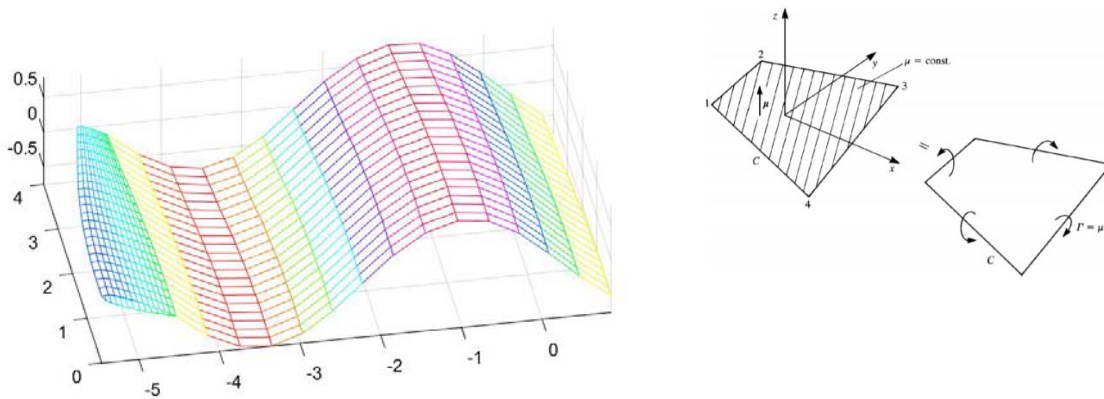


Figure 1: Discretization of a flapping wing and its trailing vortex sheet by means of quadrilateral elements carrying constant dipole strength (left), which is equivalent with vortex ring elements (right). Only the half symmetric part with respect to the centerplane of wing of $AR=8$ is shown.

The method is based on the discretization of the wing sections into number of chordwise elements for a number of spanwise sections as shown in the Fig.1 above. A scanning procedure is applied in order to define the 4 nodal points of the vortex ring elements, which then are used to calculate the influence coefficients on the collocation points (defined as the centroids of the ring elements on the body surface).

The wing undergoes an oscillatory heaving and pitching motion, with same frequency and phase difference around 90deg, while traveling at constant speed, in order to operate in a flapping mode; see Triantafyllou et al (2000, 2005). The most important parameters are the Strouhal number $Str = \omega h_0 / (\pi U_\infty)$, the heaving motion amplitude h_0/c and the pitching amplitude θ_0 , where ω is the angular frequency, and U_∞ denotes the incident parallel inflow due to the steady forward speed of the flapping thruster.

In treating time – dependent motion of bodies, the selection of the coordinate systems becomes important. It is useful to describe the unsteady motion of the wing on which the flow – tangency condition is applied in a body – fixed coordinate system (x,y,z) ; see Katz & Plotkin (1990). The motion of the origin is prescribed in an inertial frame of reference (X,Y,Z) . In the present work, the flapping wing starts from rest, and we also consider the wing to perform a pitching angle $\theta(t)$, a vertical oscillatory heaving motion $h(t)$, and thus

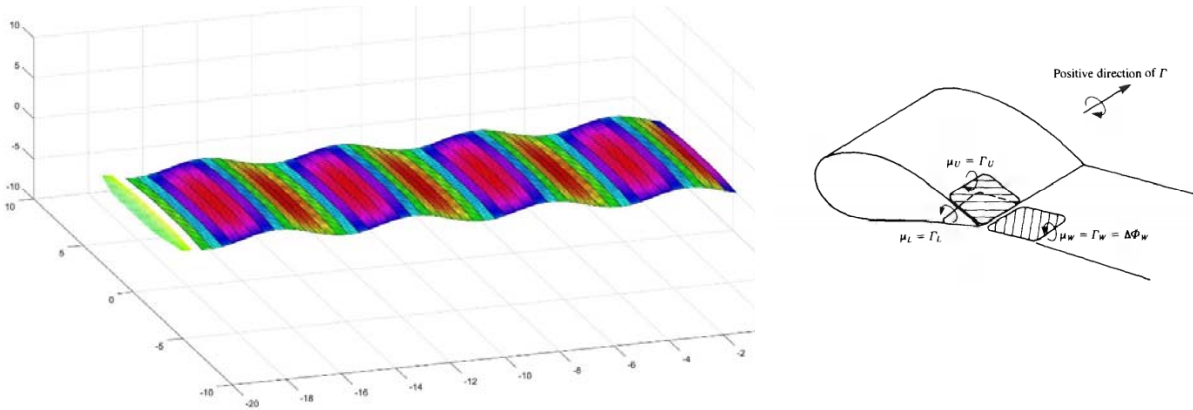


Figure 2. Vortex wake development of flapping thruster operating at a Strouhal number $Str=0.23$, with heaving amplitude with $h_0/c=0.75$ and pitching amplitude $\theta_0 = 23\text{deg}$, during 4 periods of oscillation (left), Morino – type Kutta condition (right).

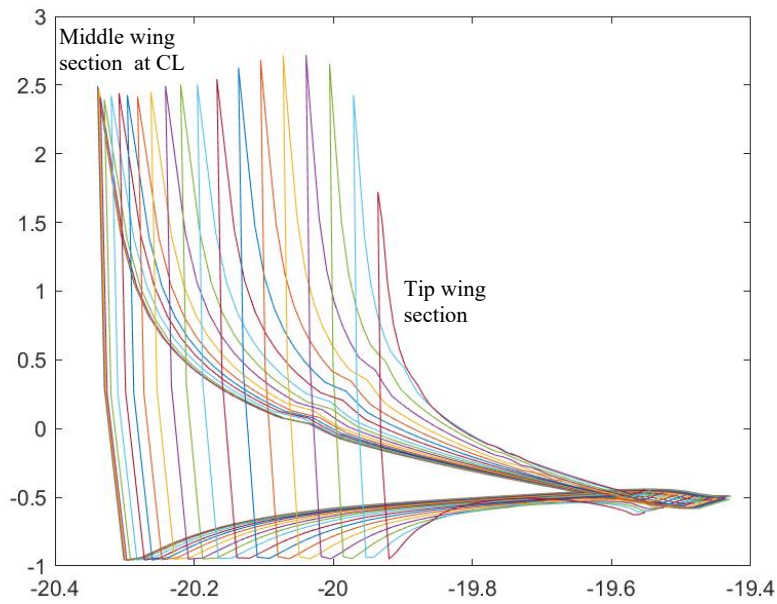


Figure 3. Pressure distribution of every wing section in the case of flapping thruster at a Strouhal number $Str=0.23$, with heaving amplitude with $h_0/c=0.75$ and pitching amplitude $\theta_0 = 23\text{deg}$.

$$\begin{aligned}
 X &= -Ut + x \cos \theta + z \sin \theta \\
 Y &= y \\
 Z &= h(t) - x \sin \theta + z \cos \theta
 \end{aligned}
 \tag{1}$$

The solution is based on a time – stepping technique, and at the beginning of the motion only the bound vortex ring elements on the unsteady thruster exist. The closing segment of the trailing – edge vortex

elements represent the starting vortex. At the first time step, there will be no wake panels. During the second time step, the wing is moved along its flight path and each trailing – edge vortex panel sheds a wake panel with a vortex strength equal to its circulation in the previous time step. This time step methodology can be continued for any type of foil path and at each time step the vortex wake corner points can be moved by the local velocity, so that the wake rollup can be simulated.

The problem is solved by calculating the influence coefficients of the induced potential and velocity F_{ij} , $\mathbf{U}_{ij} = (U_{ij}, V_{ij})$, for $i, j = 1, \dots, K$. by each vortex ring element on each collocation point on the wing, which is selected as the centroid of each quadrilateral element. The latter quantities are used to set up a linear system of equations by constructing the coefficient matrix. To this respect, the flow – tangency condition is implemented on the wing surface, requiring zero normal velocity. Consequently, in the present case, the discrete system of equations expressing the flow tangency condition at the collocation points on the wing is:

$$\sum_{k=1}^K A_{lk} \Gamma_k = \mathbf{b}_l - \mathbf{n}_l \cdot \sum_{k=1}^{K_w(t)} U_{lk}^w \Gamma_{kl}^w, \quad \text{for } l = 1, 2, \dots, K \quad , \quad (2)$$

where Γ_k are the bound vortex ring element strengths and the matrix coefficient is composed by $A_{ij} = \mathbf{n}_i \cdot \mathbf{U}_{ij}$, for $i = 1, \dots, K$, and \mathbf{n}_i , $i = 1, \dots, K$ the unit normal vector directed to the exterior of the body. In Eq.(2) k is an one – dimensional counter for each collocation point, and l for each vortex ring element. The index $K_w(t) = M \times N_w(t)$ corresponds to the number of wake panels generated by the unsteady wing motion up to the time instant t , where $N_w(t) = t / \delta t$, where δt is the time step. The system is supplemented by a Morino-type Kutta condition used to determine the vortex ring intensity in the wake element adjacent to the trailing edge is in this case connected with the ring intensities of the first element in the lower wing side and the last element in the upper wing side (see Fig. 2) as follows

$$\Gamma_w = \Gamma_{TE} = -(\mu_{upper}^{TE} - \mu_{lower}^{TE}) \quad . \quad (3)$$

The first term in the right – hand side of Eq.(2) is defined by:

$$\mathbf{b}_k = -\mathbf{u}_k \cdot \mathbf{n}_k, \quad k = 1, \dots, K, \quad (4)$$

with \mathbf{u}_k denoting the relative flow velocity at the collocation points of the wing

$$\mathbf{u} = (u_x, u_y, u_z) = U\mathbf{i} - \frac{d\theta}{dt}(\mathbf{j} \times \mathbf{r}_w) - \frac{dh}{dt}\mathbf{k} \quad , \quad (5)$$

where $\mathbf{i}, \mathbf{j}, \mathbf{k}$, are the unit vectors along the axes x, y, z respectively and \mathbf{r}_w denotes the position vector on the wing. In the right hand side of Eq.(2) the influence of the vortex-ring elements modelling the shed wake vorticity on the wing wake is included. The summation is over the $K_w = M \times N_w$ vortex elements of the wake (M in the spanwise direction and N_w in the downstream direction) which are generated from the motion of the wing, after discretization to equal time steps δt . The total potential on the surface S of the unsteady wing is approximately:

$$\Phi(s_1, s_2) = \phi(s_1, s_2) + U_\infty x \quad , \quad (6)$$

and it can be used for the calculation of the velocity on the wing by covariant differentiation of the potential in curvilinear coordinates on the wing (s_1 -cordwise and s_2 -spanwise):

$$u_1 = \frac{\partial \Phi}{\partial s_1}, u_2 = \frac{\partial \Phi}{\partial s_2}, \quad (7)$$

from which the the total velocity is estimated:

$$\mathbf{w} = u_1 \mathbf{e}_*^1 + u_2 \mathbf{e}_*^2, \quad (8)$$

where $\mathbf{e}_*^1, \mathbf{e}_*^2$ denotes the physical components of the surface contravariant base on the wing. After obtaining the velocity, the pressure distribution is calculated by applying the unsteady Bernoulli's equation providing the instantaneous distribution of the pressure coefficient

$$C_p = \frac{p - p_\infty}{1/2 \rho U_\infty^2} = 1 - \frac{|\mathbf{w}|^2}{U_\infty^2} - \frac{2}{U_\infty^2} \frac{\partial \Phi}{\partial t}. \quad (9)$$

Finally, time dependent hydrodynamic responses concerning flapping thruster forces and moments are calculated by pressure integration over the wing surface. Indicative results are presented in Figs 2 and 3 as obtained by the present method.

3 Comparison with unsteady hydrofoil theory

In this section results from the present 3D unsteady panel method are compared against unsteady hydrofoil theory by Theodorsen (1935) and experimental data from Schouveiler et al (2005).

The case of flapping wing of large aspect ratio of Fig.2 is studied for verification. Using Theodorsen theory (see Katz & Plotkin 1990) in the case of wings of finite aspect ratio the lift force F_L can be estimated as:

$$F_L = \frac{1}{2} \pi \rho U A H (AR) C(k) \left[U \theta - \dot{h} + \left(\frac{3}{4} - \frac{p}{c} \right) c \dot{\theta} \right] + \frac{\pi \rho c^2}{4} \left[(U \dot{\theta} - \ddot{h}) + c \left(\frac{1}{2} - \frac{p}{c} \right) \ddot{\theta} \right], \quad (10)$$

where p/c is pitching axis location, $k = \omega c / (2U)$ is the reduced frequency $C(k)$ is the Theodorsen function (lift deficiency factor), A is the area of the foil, and $H = AR (AR + 2)^{-1}$ is a 3D correction from lifting – line theory (elliptic wing). In Fig.4 at the top subplot the time-history of foil angle of attack $\alpha(t)$ shown for a time interval of 4 periods,

$$a(t) = \theta(t) - a_b(t), \quad \text{where } a_b(t) = \tan^{-1} \left(\frac{\dot{h}}{U} \right) \quad (11)$$

where the foil pitching and heaving oscillatory motions are defined as follows

$$\theta(t) = \theta_0 \sin(\omega t + 0.5\pi) \text{ and } h(t) = h_0 \sin(\omega t). \quad (12)$$

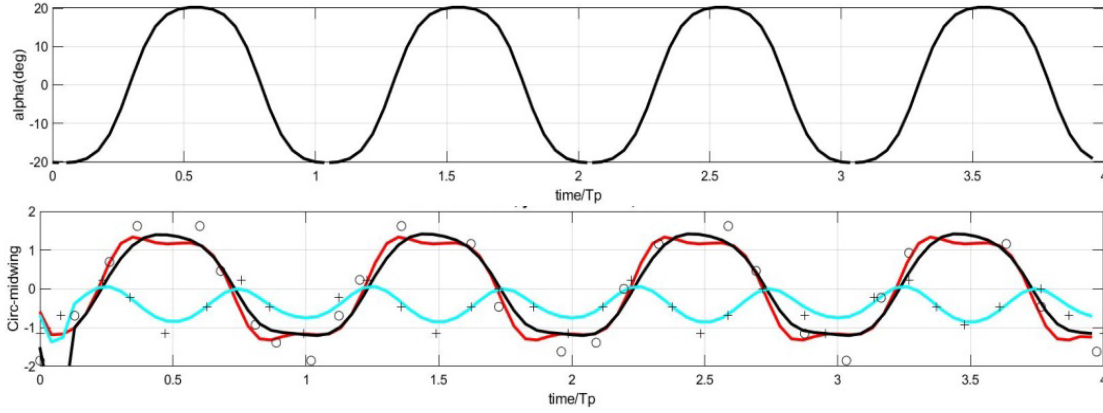


Figure 4. Comparison of present method prediction with Theodorsen's unsteady hydrofoil theory and experimental data by by Schouveiler et al (2005) in the case of foil of $AR=6$, at $Str=0.23$, $h_0/c=0.75$, $\theta_0 = 23\text{deg}$. Top subplot: angle of attack $\alpha(t)$. Lower subplot: Lift and thrust coefficients as calculated by the present method and compared with theory (red line) and measured data (symbols).

In the last subplot the vertical (lift) force coefficient is shown by using black line and the horizontal (thrust) force by using cyan line, as calculated by the present method, and are compared against the measured data shown by using symbols and the unsteady hydrofoil theory results by using red lines. It is observed that the present method provides compatible predictions concerning the integrated quantities with unsteady hydrofoil theory and the experiment approximating satisfactorily the maxima of both the lift and thrust forces.

4. Flapping thruster noise prediction

As the flapping thruster operates, it is subjected mainly to unsteady pressure loads. Low frequency noise is caused by the fluctuations of foil pressure and volume flow disturbance due to oscillatory motion. The usual formulation for the acoustic pressure p' generated from rotating machinery is based on the Ffowcs Williams and Hawkings (1969) equation as follows

$$\frac{1}{c^2} \frac{\partial^2 p'}{\partial t^2} - \nabla^2 p' = m + d + q, \quad (13)$$

where c is the speed of sound in the medium ($c=1500\text{-}1550\text{m/s}$ for water) and the various terms in the right-hand side correspond to the acoustic monopole, dipole and quadrupole source terms (Farassat & Myers 1988). The quadrupole term becomes important for strongly transonic flow phenomena at higher frequencies. Taking into account that the speed of sound in water is much greater than the flow velocities, and focusing on the low-frequency part of the generated noise spectrum the contributions by the latter term are neglected in the present work. Farassat (2001) formulation is employed offering an integral representation of the solution of Eq.(13) forced by the monopole and dipole terms. The acoustic pressure field is accordingly given by thickness and loading components, as follows

$$p'(\mathbf{x}_0, t) = p'_T(\mathbf{x}_0, t) + p'_L(\mathbf{x}_0, t) . \quad (14)$$

The loading term is given by

$$4\pi p'_L(\mathbf{x}_0, t) = -\frac{1}{c} \frac{d}{dt} \int_{f=0} \left[\frac{dp \mathbf{n} \hat{r}}{r(1-M_r)} \right]_{ret} dS + \int_{f=0} \left[\frac{dp \mathbf{n} \hat{r}}{r^2(1-M_r)} \right]_{ret} dS, \quad (15)$$

where $f=0$ indicates the moving surfaces u_n the corresponding normal velocity, where dp denotes the pressure jump on the blade surface, M_r denotes Mach number in the r -direction and the integrand is calculated at retarded time. For relatively large distances (of the order of several propeller diameters) of the observation point from the propeller, we use the approximation

$$r = |\mathbf{x}_0 - \mathbf{x}| \approx |\mathbf{x}_0 - \mathbf{x}_T(t)|, \quad \hat{r} \approx (\mathbf{x}_0 - \mathbf{x}_T(t)) / r$$

where $\mathbf{x}_T(t)$ denote the center of lift and thrust force on the flapping wing. Using the fact that the Mach number is very small, Eq.(18) leads to the following simplification

$$p'_L(\mathbf{x}_0, t) = -\frac{1}{4\pi c} \frac{dF(t_r)}{dt} \frac{x_P - x_T(t_r)}{r^2} + \frac{1}{4\pi} F(t_r) \frac{x_P - x_T(t_r)}{r^3}, \quad (16)$$

where $F(t_r)$ denotes the fluctuating unsteady part of the foil force, mainly composed from vertical (lift) and horizontal (thrust) forces, and $t_r = r/c$ denotes the retarded time between the observation point \mathbf{x}_0 and the disturbance generating point \mathbf{x}_T .

Similarly for the thickness effect we have

$$p'_T(\mathbf{x}_0, t) = \frac{\rho}{4\pi} \frac{\partial}{\partial t} \int_{f=0} \left[\frac{u_n}{r(1-M_r)} \right]_{ret} dS, \quad (17)$$

which is approximated by

$$p'_T(\mathbf{x}_0, t) \approx \frac{\rho}{4\pi} \frac{d^2 Q_c(t_r)}{dt^2} \frac{1}{|\mathbf{x}_0 - \mathbf{x}_Q(t_r)|}, \quad (18)$$

where $\mathbf{x}_{Q,k}(t)$ denotes the center of volume Q_c displaced by the foil. In the case of an unsteady cavitating foil thruster the latter term will include also the bubble cavitation volume.

Indicative results obtained by the above simplified model are presented in Fig.5 in the vicinity of the flapping thruster and at large distances. The acoustic field generated by the flapping thruster of middle chord $c=1\text{m}$ and $AR=6$ operating in the same as before conditions in water ($c=1500\text{m/s}$) is presented in Fig. 5 as calculated by the present method. Results are presented at a time instant after 3.7 periods of oscillation, starting from rest. The contribution of the monopole and the dipole term, which is dominant in the examined case, are clearly observed. In the examined case since the foil flow is not cavitating and the intensity of the acoustic field is very small. Future work will be directed to the incorporation of unsteady cavitation effects which are expected to be important in the case of flapping thrusters operating near the free surface.

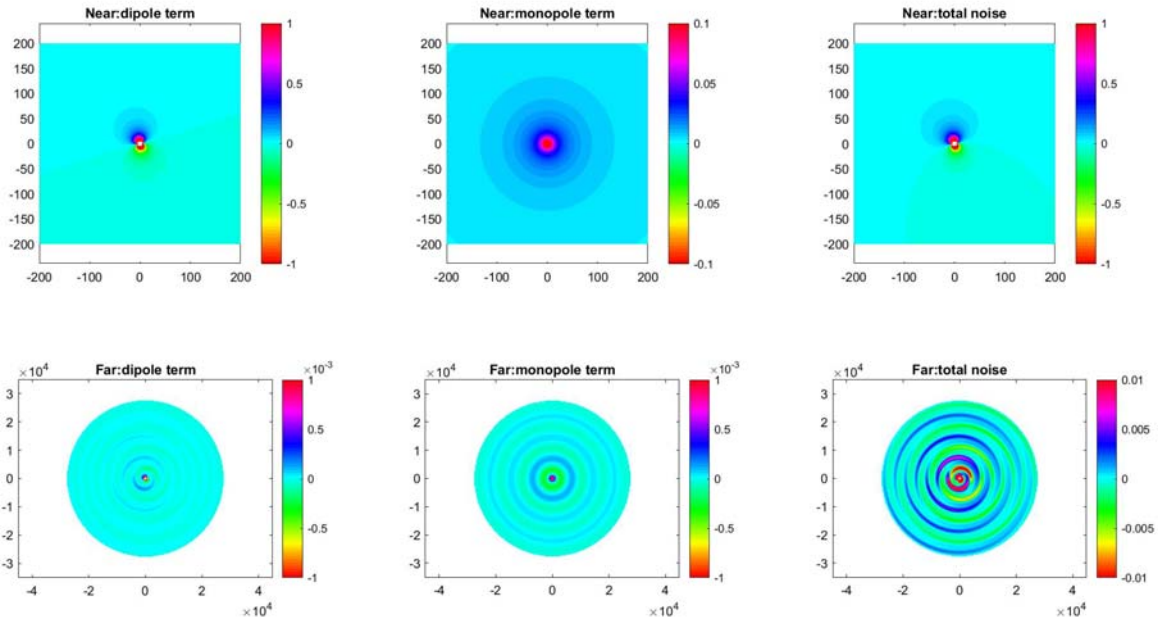


Figure 5. Calculation of acoustic field generated by the flapping thruster operating in water ($c=1500\text{m/s}$), in the case of foil of Fig.4 of $AR=6$, flapping at $St=0.23$, $h_0/c=0.75$, $\theta_0 = 23\text{deg}$, using the calculated hydrodynamic loads by the present method. Top subplot: near field from dipole and monopole term and total acoustic field in the vicinity of the flapping thruster. Lower subplot: calculated field at large distances.

5. Conclusions

In the present work a 3D vortex – ring element method has been presented for calculating the flow over wings in unsteady conditions with application to the performance of flapping thrusters operating at low Strouhal numbers. The method is shown to provide compatible predictions with unsteady hydrofoil theory and experimental data. Next, a simplified model is presented for the prediction of the hydrodynamically generated noise, based on data concerning the noise sources on the dynamic foil, coupled with the solution of the hydroacoustic problem. The present model will be used, in conjunction with methods allowing for the calculation of acoustic propagation for calculating spatial evolution of the noise spectrum, for comparative studies with the noise from standard marine propellers. An important fact is that the utilization of the flapping thruster to augment ship propulsion could enhance the combined ship/AUV propulsive performance dropping at the same time the power feed of marine propeller and reducing the overall generated noise level. Future work will be directed to the incorporation of cavitation effects which are expected to be important in the case of flapping thrusters operating at low submergence depths, including biomimetic flapping thrusters that are currently studied for augmenting ship propulsion in waves. Also, the reflection and scattering effects by the vessel or AUV hull surface and the refraction effects due to variable sound speed profile on longer-distance acoustic propagation characteristics will be considered.

Acknowledgements

The present work has been supported by Seatech H2020 project received funding from the European Union's Horizon 2020 research and innovation program under the grant agreement No 857840. The opinions expressed in this document reflect only the author's view and in no way reflect the European Commission's opinions. The European Commission is not responsible for any use that may be made of the information it contains.

6. References

- [1] Duarte C.M., et al, The soundscape of the Anthropocene ocean, *Science* Vol. 371, Issue 6529, 2021.
- [2] McKenna M.F., Ross D., Wiggins S.M., Hildebrand J.A., Underwater radiated noise from modern commercial ships, *J Acoust Soc Am.* , Vol.131, 2012, pp. 92-103.
- [3] IMO 2014. Guidelines for the Reduction of Underwater Noise from Commercial Shipping to Address Adverse Impacts on Marine Life – non mandatory technical advices, International Maritime Organization (2014) MEPC.1/Circ.833.
- [4] IMO 2008. 72nd session of the Marine Environment Protection Committee (MEPC 70) at the International Maritime Organization.
- [5] Belibassakis K., 2018, A velocity-based BEM for modeling generation and propagation of underwater noise from marine propellers, Proc. Euronoise 2018, Hersonissos Crete.
- [6] Seol H., Suh J.C., Lee S., Development of hybrid method for the prediction of underwater propeller noise, *Journal of Sound and Vibration* Vol.288, 2005, pp.345–360.
- [7] Triantafyllou M.S., Triantafyllou G.S., Yue D.K.P., Hydrodynamics of fishlike swimming. *An. Review Fluid Mech.* Vol.32, 2000.
- [8] Rozhdestvensky K.V., Ryzhov V.A. 2003, Aero-hydrodynamics of flapping wing propulsors. *Progress in Aerospace Sciences* Vol.39, 585-633.
- [9] Triantafyllou M.S., Hover F.S., Techet A.H., Yue D.K.P., 2005, Review of hydrodynamic scaling laws in aquatic locomotion and fishlike swimming, *Journal of American Society of Mechanical Engineers* Vol.58, 226.
- [10] Belibassakis K.A. & Politis G.K.. Hydrodynamic performance of flapping wings for augmenting ship propulsion in waves. *Ocean Engineering* Vol.72, 2013, pp.227 – 240.
- [11] Belibassakis K.A., Filippas E.S., Ship propulsion in waves by actively controlled flapping foils. *Applied Ocean Research* Vol.52, 2015, pp.1-11.
- [12] Wu, X., Zhang, X., Tian, X., Li, X., Lu, W., A review on fluid dynamics of flapping foils. *Ocean Engineering* Vol.195, 2020, 106712.
- [13] Katz J., Plotkin A., 1990. *Low-speed aerodynamics*. Volume 13. Cambridge University Press.
- [14] Schouveiler, L., Hover, F.S. and Triantafyllou, M.S. (2005), *Performance of flapping foil propulsion*, *J. Fluids and Structures* 20, pp. 949-959.
- [15] Theodorsen, T. 1935, *General Theory of Aerodynamic Instability and the Mechanisms of Flutter*, NACA Report No. 496; National Advisory Committee for Aeronautics: Washington, DC, USA, 1935.
- [16] Ffowcs Williams, J. E. and Hawkings, D. L., Sound Generated by Turbulence and Surfaces in Arbitrary Motion, *Philosophical Transactions of the Royal Society*, Vol. 264, No. 1151, 1969, pp. 321–342.
- [17] Farassat F and Myers M. K. , “Aerodynamics Via Acoustics: Application of Acoustic Formulas for Aerodynamic Calculations,” AIAA 86-1877, 1986.
- [18] Farassat, F., Acoustic radiation from rotating blades – the Kirchhoff method in aeroacoustics. *Journal of Sound and Vibration* Vol. 239 2001, pp.785-800.